International Journal of
Science Inventions Today
www.ijsit.com
ISSN 2319-5436
Research Article

INVESTIGATION OF MORPHOLOGICAL CHARACTERISTICS OF CORONARY BIFURCATION CORE IN NORMAL SUBJECTS WITH CCTA

*Diljan Mansoor and Prof. Dr. Liang Long Chen

Fujian Medical University Union Hospital, Fuzhou, China

ABSTRACT

Background: Coronary bifurcation lesions (CBLs) account for approximately 15-20% cases of percutaneous coronary intervention (PCI) and remain a challenging lesion subset for cardiac interventionists. As compared to non-CBLs, PCI of CBLs was associated with poorer clinical outcomes in terms of major adverse cardiac events (MACE) particularly target lesion failure (TVF)

Objectives: To set up a method to detect BFC/POC shape and to its dimension in different bifurcation types and locations; to validate the four models based on the coronary bifurcation measurement from normal population; to investigate potential relevance of the BFC/POC morphology in CBLs interventions.

Methods:

Inclusion criteria:

1. subjects with unknown chest discomfort in whom coronary artery disease could be finally excluded clinically,
2. subjects underwent CCTA with normal or negative findings either by CCTA or invasive coronary angiography if obtainable,
3. images of CCTA with high-quality.

Exclusion criteria:

1. subjects with unknown chest discomfort in whom coronary artery disease couldn't be finally excluded clinically,
2. any detectable lesions in any bifurcated segments by CCTA,
3. suboptimal images of CCTA.

Result: A total of 200 subjects eligible were included in this study with measurable bifurcations located at different bifurcation types and location including the distal LM of 200.

Distribution at both side branch at PMV and POC, re directing the significant important. Normal coronary bifurcation measurement in the different segment bifurcations.

For coronary bifurcation core and for distal LM bifurcation the best rule was Finet whose vessels diameters obey Finet rule.

The mother vessel diameter calculated with the HK rule or Murray is either bigger or smaller than that measured with professional software of CCTA.

Conclusion: For more accurate description of the relationship among three bifurcated segments: for the Y-type and T-type, the best rule was finet types for both bifurcations whose vessels diameter and bifurcation angles obey finet rule. The mother vessel diameter calculated with the HK rule or Murray is either bigger or smaller than that measured with professional software of CCTA. For bifurcations of the distal LM, LAD-Dx, LCX-OMx, and distal RCA, the best rule was finet type whose vessels diameter and bifurcations angel obey finet diameter rule. The bifurcations from coronary artery were found to obey the finet diameter model and angle rule much more than HK and Murray's model. For distal LM bifurcation the best rule was Finet whose vessels diameters obey Finet rule.

Keywords: Percutaneous coronary intervention (PCI), Computed Tomography Coronary Angiography (CCTA), CT, Polygon of confluence (POC), Coronary Bifurcation Core (BFC), Coronary artery disease (CAD)

INTRODUCTION

Coronary bifurcation lesions (CBLs) account for approximately 15-20% cases of percutaneous coronary intervention (PCI) and remain a challenging lesion subset for cardiac interventionists. As compared to non-CBLs, PCI of CBLs was associated with poorer clinical outcomes in terms of major adverse cardiac events (MACE) particularly target lesion failure (TVF) [1, 2]. There were numerous causes attributable to the unfavorable outcomes but the major one may be the failure to restore the native bifurcated morphology by current PCI techniques. Hence, investigation of bifurcated anatomy or/and improvement of PCI techniques are of great clinical relevance. Percutaneous coronary intervention (PCI) attempts to restore the lumen area of a diseased artery to "normal" reference dimension through percutaneous transluminal coronary angioplasty (PTCA) or stenting. As atherosclerosis often stems from the junction of a bifurcation and diffuses over the vessel length the question becomes what is the therapeutic target diameter of the diseased vessel to restore flow optimality to a bifurcation. In other words, if the diameters of two segments of a "normal" bifurcation are known, can an optimal diameter of the third segment be determined to ensure an optimal flow through the bifurcation? has long been established that there is an optimal relationship between the diameters of the three segments of a bifurcation. Table 1 lists the most commonly referenced bifurcation models that provide a mathematical relationship between the three segments of a bifurcation (i.e., D_m, D_l and D_s for the diameters of mother, large and small daughters, respectively). In 1926, Murray was the first to derive a cubed relationship between the mother and two daughter vessels. The premise of Murray's derivation is the minimum energy hypothesis; i.e., the power for transport of blood through a bifurcation is minimized. This is the principle of efficiency where departure from which requires greater energy dissipation. Huo and Kassab[7] recently showed a similar relationship based on the same premise in a tree structure, but found an exponent instead of 3 in the

Murray model. Finet proposed an empirical fractal-like rule. An additional expression stemming from area conservation (exponent of 2) has traditionally been invoked for the vasculature. The objective of this study is to validate the four models (Table 1) based on the coronary bifurcation measurement from normal population. The most accurate rule based on a physical and physiological principle can then be used to determine the desired diameter segment when the diameters of the two other segments in a bifurcation are known for percutaneous treatment.

Rationale:

A bifurcation vessel is composed mainly by 3 segments (proximal main vessel, PMV; distal main vessel, DMV; and side branch, SB), 3 bifurcated angles and 1 bifurcated core (BFC) where the 3 segment connect each other, encompassing an area, the polygon of confluence (POC) and 1 carina. Also, a bifurcation vessel can be categorized by 2 types (T- or Y-type) according to the distal bifurcated angle (DBA) of ≥70° or <70°.

It has long been established that there is an optimal relationship among the diameters of the three segments of a bifurcation [3]. As listed in the Table 1, the most commonly referenced bifurcation models that provide a mathematical relationship between the three segments of a bifurcation (DM, DL and DS for the diameters of mother, large and small daughters, respectively). In 1926, Murray was the first to derive a cubed relationship between the mother and the two daughter vessels, so-called Murray's rule [4]. The premise of Murray's derivation is the minimum energy hypothesis; i.e., the power for transport of blood through a bifurcation is minimized. This is the principle of efficiency where departure from which requires greater energy dissipation. Huo and Kassab recently showed a similar relationship based on the same premise in a tree structure, but found an exponent instead of 3 in the Murray model [5]. Finet proposed an empirical fractal-like rule, greatly facilitating clinical practice [6].

Murray's rule and the associated rules have been broadly adopted for guidance of CBLs interventions. For an instance, if the "normal" or reference diameters of two segments of a bifurcation are known, an optimal diameter of the third segment can be determined to ensure an optimal flow through the bifurcation, which is very useful for properly selecting of interventional devices. Besides, Murray's rule can be used for optimization of CBLs interventions, such as selection of the suitable balloon size for proximal optimization treatment or final kissing balloon dilation. Moreover, Murray's rule can also be used for prediction of bifurcated restenosis or MACE following CBLs intervention. For example, Kang J et al. found a rule of "5-6-7-8" for prediction of restenosis and re-PCI of distal LM CBLs [7]. However, there are several issues not addressed whether Murray's rule and the associated rules are adapted to the BFC or POC[8]., or not clearly state whether all the rules have an equal power to descript the relationship among the bifurcated segments in different types of bifurcations.

Bifurcation diameter models	Relationship	Physical mechanisms
HK	$D^{7/3\,PMV} = D^{7/3\,DMV} + D^{7/3\,SB}$	Minimum energy
Finet	Dm=0.678 × (Dl+Ds)	‘’Fractal’’-type relation
Murray	D 3m = D 3l + D 3s	Minimum energy and WSS-Constant
Area Preservation	D 2m = D 2l + D 2s	Velocity-constant

Table 1: Bifurcation diameter models and the corresponding physical mechanisms

where D_m, D_l, and D_s are the diameters of mother, larger and smaller daughter vessels, respectively.

A coronary bifurcation lesion [9]. occurs at or near a division of a major coronary artery. Characterizing bifurcation lesions involves assessing the lesion morphology in three important anatomic segments: (1) proximal main branch (MB); (2) distal MB; and (3) side branch (SB).

The carina is the inflection point at which the proximal MB bifurcates into the distal MB and SB. The European Bifurcation Club defines a bifurcation lesion as a significant stenosis (i.e., >50%) in a coronary artery adjacent to and/or involving the origin of an SB that is clinically significant.

Numerous classification schemes have been proposed to characterize coronary bifurcation lesions [2.1]. The simplest and most widely used is the Medina classification. The Medina classification assesses plaque burden based on the presence (“1”) or absence (“0”) of stenosis in the proximal MB, distal MB, and SB (Figure 1).

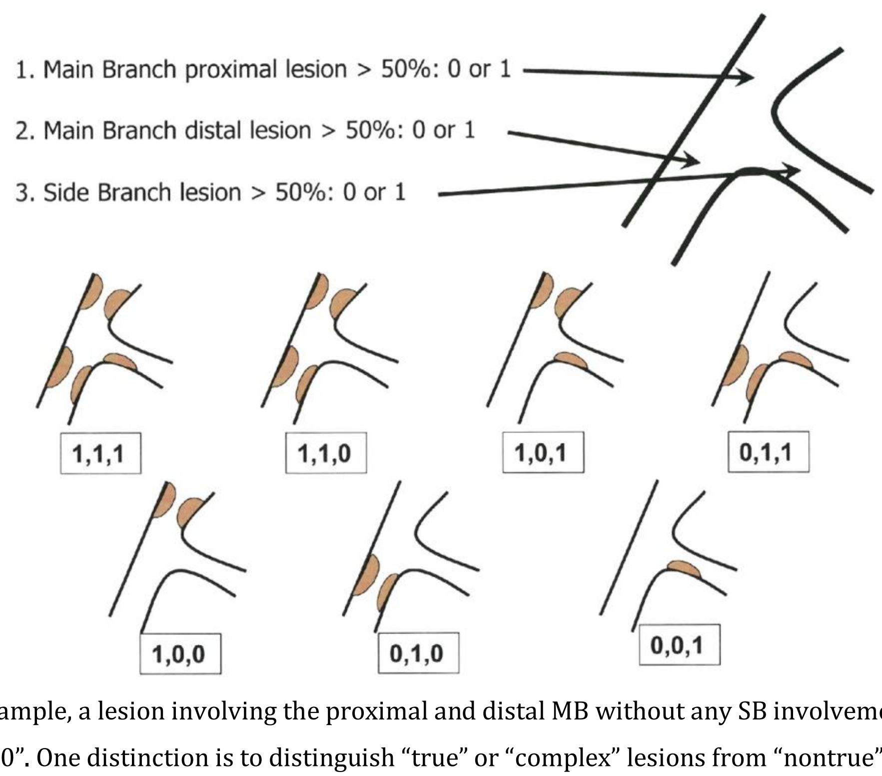

Figure 1: For example, a lesion involving the proximal and distal MB without any SB involvement is classified as Medina “1,1,0”. One distinction is to distinguish “true” or “complex” lesions from “nontrue” or “pseudo-” bifurcation lesions.

A "true" bifurcation lesion involves significant (>50%) stenosis in both the MB and the SB (i.e., Medina 1,1,1; 1,0,1; or 0,1,1), whereas all other lesion types would be classified as "nontrue." It is important to recognize that angiography may be limited in terms of its ability to appropriately classify bifurcation lesions, and adjunctive modalities such as intravascular ultrasound (IVUS) may be necessary to determine a lesion's true classification.

Among patients with chest pain without significant coronary artery disease, coronary artery spasm (CAS), myocardial bridge (MB), and/or insignificant coronary stenosis (ICS) have been frequently found.

From a long-term clinical evaluation of patients without coronary artery disease, aging and ICS were strongly associated with major adverse cardiac events. Further, aging, dyslipidemia, ICS, CAS, and MB were strongly associated with sustained angina pectoris. Additionally, when clinicians are evaluating the cause of chest pain, it may be judged to be cardiovascular if the physician suspects the presence of CAS, MB, and ICS despite absence of significant coronary artery disease. In particular, CAS, MB, and ICS may exist independently but could also appear in combination with one another. The combination of CAS, MB, and/or ICS was associated with poor long-term clinical outcomes compared with single factors. The presence of ICS was the strongest independent predictor for major adverse cardiac events and sustained angina pectoris; therefore, patients with chest pain and ICS should be carefully treated and need close clinical follow-up, even in the absence of significant coronary artery disease.

Chest pain is a major symptom of ischemic heart disease such as angina pectoris (AP) and acute coronary syndrome (ACS); [10,11]. therefore, it is important to identify and diagnose the causes of pain in these patients. The main mechanism of AP is the imbalance between oxygen demand and supply in the myocardium. Obstructive coronary stenosis, coronary artery spasm (CAS), and myocardial bridge (MB) are well-known causes of myocardial ischemia. [10.11.12.13.14.15.17]. CAS is a well-known endothelial dysfunction, and MB is substantially implicated in a high incidence of CAS; thus, both MB and CAS are major causes of vasospastic angina. [11,12]. Therefore, if the cause of chest pain is judged to be cardiovascular, clinicians usually evaluate coronary arteries with electrocardiography, stress test, cardiac computed tomography scans, and coronary angiography, (CAG) including the intracoronary acetylcholine (ACH) or ergonovine provocation test. [11]. Obstructive coronary stenosis requires active treatment with mechanical revascularization and drug intervention, as it is known to be closely related to poor prognoses such as ACS, myocardial infarction (MI), and death.[1] However, if no significant coronary lesion is seen on CAG despite chest pain, the scope of determining the prognosis and its association are limited.

BACKGROUND

Cardiovascular disease (CVD) [18]. is a class of diseases that involve the heart or blood vessels. CVD includes coronary artery diseases (CAD) such as angina and myocardial infarction (commonly known as a heart attack). Other CVDs include stroke, heart failure, hypertensive heart disease , rheumatic heart disease, cardiomyopathy, heart arrhythmia, congenital heart disease, valvular heart disease, carditis, aortic aneurysms, peripheral artery disease, thromboembolic disease, and venous thrombosis.

Cardiovascular disease is the leading global cause of death, accounting for an estimated 17.5 million deaths in 2012, and coronary artery disease represented 42 % of these deaths.

Percutaneous Coronary Intervention is a non-surgical procedure that uses a catheter to place a small structure called a stent to open up blood vessels in the heart that have been narrowed by plaque buildup, a condition known as atherosclerosis.

However, in-stent restenosis of bare metal stents (BMS) and late thrombosis of drug-eluting stents (DES) are important limitations of coronary stenting today with poor stent expansion being a predictor of restenosis.

Both stent over-sizing and under-sizing can have detrimental effects. Larger stents induce more trauma to vessels and can lead to coronary dissection and/or rupture Under expanded or undersized stents increase the risk of both restenosis and the likelihood of stent thrombosis. It is therefore important for the cardiovascular community to understand and quantify the anatomy of the coronary vessels, in particular, that of bifurcations where atheromatous narrowing is common. In the China, there were an estimated 954,00000 PCI [19]. procedures in 2010. In a large European study with nearly 100,000 stent deployments, restenosis rates were estimated at 7.4 % for BMS and up to 5.8 % for DES. With the advent of computational atlasing and associated tools, we can deliver an innovative and accurate database to assist in the informed improvement of stent technology. The aims of this study are therefore to characterize the coronary anatomy for future stent design, and to establish a large *normal* database of cases to which future models with disease can be compared. Most studies in the literature rely on anatomical measures derived from patients with established disease, use suboptimal two-dimensional projection imaging techniques, and suffer from high inter observer variability (e.g. Previously, we published selected basic measures such as angles and diameters. In this work, we present a computer- aided design (CAD) [20]. to a correspond population of shapes, and apply it to build a large expert-reviewed fully 3D atlas of vessel bifurcations. This atlas allows us to test for shape differences in a holistic fashion by using clinical risk factors. Heart disease is the leading cause of death among men and women in the United States. Coronary artery disease affects 16.5 million Americans. The American Heart Association (AHA) estimates that someone in the US has a heart attack about every 40 seconds. In addition, for patients with no risk factors for heart disease, the lifetime risk of having cardiovascular disease is 3.6% for men and less than 1% for women. Having 2 or more risk factors increase the lifetime risk of cardiovascular disease to 37.5% for men and 18.3% in women.

Unstable angina: This may be a new symptom or a change from stable angina. The angina may occur more frequently, occur more easily at rest, feel more severe, or last longer. Although this can often be relieved with oral medications (such as nitroglycerin), it is unstable and may progress to a heart attack. Usually, more intense medical treatment or a procedure is required to treat unstable angina.

Non-ST segment elevation myocardial infarction (NSTEMI): This type of heart attack, or MI, does not cause major changes on an electrocardiogram (ECG). However, chemical markers in the blood indicate that damage has occurred to the heart muscle. In NSTEMI, the blockage may be partial or temporary, so the extent of the damage is usually relatively small.

ST segment elevation myocardial infarction (STEMI): This type of heart attack, or MI, is caused by a sudden blockage in blood supply. It affects a large area of the heart muscle and causes changes on the ECG as well as in blood levels of key chemical markers.

Although some people have symptoms that indicate they may soon develop acute coronary syndrome, some may have no symptoms until something happens, and still, others have no symptoms of acute coronary syndrome at all.

Ischemia is a condition described as "cramping of the heart muscle." Ischemia occurs when the narrowed coronary artery reaches a point where it cannot supply enough oxygen-rich blood to meet the heart's needs. The heart muscle becomes "starved" for oxygen-rich blood to meet the heart's needs. The heart muscle becomes "starved" for oxygen.

Ischemia of the heart can be compared to a cramp in the leg. When someone exercises for a very long time, the muscles in the legs cramp up because they're starved for oxygen and nutrients. Your heart, also a muscle, needs oxygen and nutrients to keep working. If the heart muscle's blood supply is inadequate to meet its needs, ischemia occurs, and you may feel chest pain or other symptoms.

Ischemia is most likely to occur when the heart demands extra oxygen. This is most common during exertion (activity), eating, excitement or stress, or exposure to cold.

When ischemia is relieved in less than 10 minutes with rest or medications, you may be told you have "stable coronary artery disease" or "stable angina." Coronary artery disease can progress to a point where ischemia occurs even at rest.

Ischemia and even a heart attack can occur without any warning signs and is called "silent" ischemia. Silent ischemia can occur among all people with heart disease, though it is more common among people with diabetes. **Non-modifiable risk factors** (those that cannot be changed) include: **Male gender**. Men have a greater risk of heart attack than women do, and men have heart attacks earlier in life than women. However, beginning at age 70, the risk is equal for men and women. **Advanced age.** Coronary artery disease is more likely to occur as you get older, especially after Age 65. **Family history of heart disease**. You have an increased risk of developing heart disease if you have a parent with a history of heart disease, especially if they were diagnosed before Age 50. Ask your doctor when it's appropriate for you to start screenings for heart disease so it can be detected and treated early. **Race**. African Americans have more severe high blood pressure than Caucasians and, therefore, have a higher risk of heart disease. The risk of heart disease is also higher among Mexican Americans, American Indians, native Hawaiians, and some Asian Americans. This is partly due to higher rates of obesity and diabetes in these populations. **Modifiable risk factors** (those you can treat or control) include: Cigarette **smoking** and exposure to tobacco smoke **High blood cholesterol and high**

triglycerides – especially high LDL ("bad") cholesterol over 100 mg/dL and low HDL ("good") cholesterol under 40 mg/dL. Some patients who have existing heart or blood vessel disease, and other patients who have a very high risk, should aim for an LDL level less than 70 mg/dL. Your doctor can provide specific guidelines. **High blood pressure** (140/90 mmHg or higher) Uncontrolled **diabetes (HbA1c >7.0) Physical inactivity** Being **overweight** (body mass index [BMI] 25–29 kg/m2) or being obese (BMI higher than 30 kg/m2)

Hypotheses:

We hypothesize that the different located bifurcations and morphology of BFC/POC may not abide Murray's rule or the associated rules.

Objectives:

This study aims: 1) to set up a method to detect BFC/POC shape and to its dimension in different bifurcation types and locations; 2) to validate the four models based on the coronary bifurcation measurement from normal population; 3) to investigate potential relevance of the BFC/POC morphology in CBLs interventions.

MATERIALS AND METHODS

Sample Data:

In this study Computed tomographic angiography (CTCA) is routinely used in the assessment of coronary heart disease due to its superior resolution compared with other imagining modalities. All datas were collected from CTCA lab database (Fuzhou union hospital, department of Cardiology) with the consent from Dr Chen. All the patients included here are with zero calcium score, no stenosis, HTN and DM is not associated with size and angels of coronary bifurcation.

We used CTCA atlas to assess the POC for distal LM. Four segments within 90 LM bifurcation were (1) ostial LAD, (2) POC, and (3) distal LM (DLM)--from LAD and (4) ostial LCX.

A population N= 200 with no stenosis, zero calcium score and no intermediate artery was retrospectively selected from our CTCA database. The population demographics were 67% male and 33% female, the youngest patient is 41 and oldest one is 85.

Study population:

Inclusion criteria:

1. subjects with unknown chest discomfort in whom coronary artery disease could be finally excluded clinically.
2. subjects underwent CCTA with normal or negative findings either by CCTA or invasive coronary angiography if obtainable.
3. images of CCTA with high-quality.

Exclusion criteria:

1. subjects with unknown chest discomfort in whom coronary artery disease couldn't be finally excluded clinically.
2. any detectable lesions in any bifurcated segments by CCTA.
3. suboptimal images of CCTA.

CCTA imaging:

Coronary computed tomography angiography (CCTA) was performed by using a multi-slice CT scanner (Evolution, GE Healthcare, optima CT660, USA) with ECG-gated during total cardiac circle for coronary artery imaging. Basilica vein was punctured for a bolus injection of 1.0 ml/kilogram of iodic contrast medium. Imagining raw data was digitally stored in a workstation incorporated with specialized analytic software (Software for Evolution, GE Healthcare, optima CT660, USA) to subsequently reconstruct and analyze 2-and 3-dimensional images.

CCTA analysis:

Target bifurcation for measurement:

1. All bifurcations, either T-type or Y-type bifurcation, were deemed to be candidates of the target bifurcations.
2. The target bifurcations could be located at the distal LM (LM-LAD-LCX), LAD-Dx, LCX-OMx, or distal RCA (RCA-PDA-PL) bifurcations.
3. The SB diameter should be ≥2.5mm;

Build-up measuring models:

1. POC definition: firstly drawing the centerlines of each bifurcated segment respectively, and then the lines from the carina level perpendicular to the centerline of DMV and SB (served as DMV and SB diameter or two of the bottom margin of POC); step-by-step measuring PMV diameter along PMV centerline at 1.0 mm step-size until the diameter abruptly increases by 0.25mm bigger than PMV reference diameter to identify the beginning of the bifurcated core.
2. For Y-type bifurcation, there is a polygon area connecting each bifurcated segment (BFC/POC) which was encompassed by 5 margins (Figure-1), whereas for T-type bifurcation, there is a trapezoid area rather than a POC in the bifurcated core.

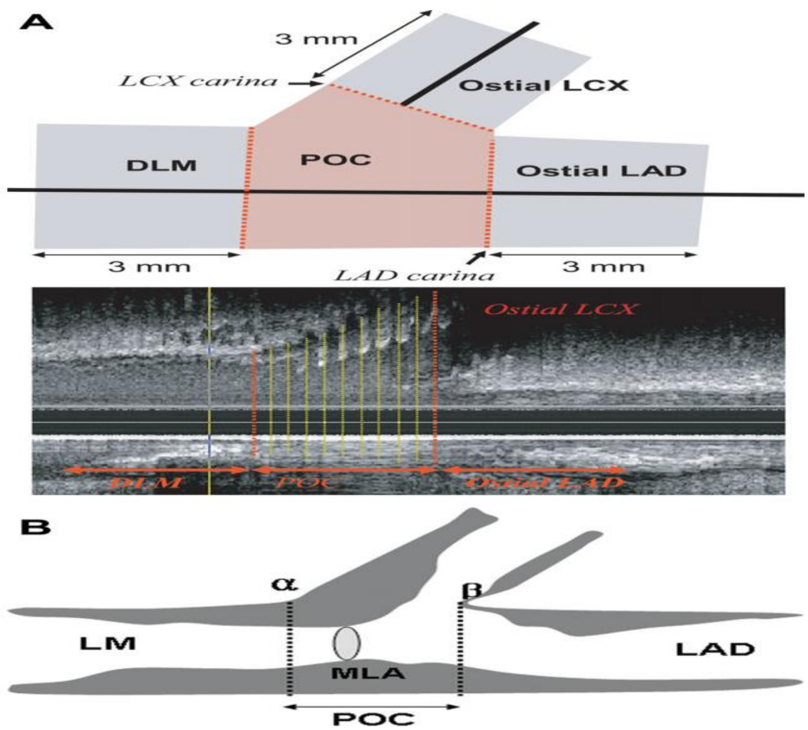

Figure 2: Definition of the polygon of the confluence in the bifurcated core for the Y-type bifurcations

Parameters for measurements:

1. Distal bifurcation angle (DBA): measured in the end-diastole at the best projection plane of the different bifurcations.
2. Dimensions: (1) each marginal length of POC including the diameter of PMV, DMV and SB, and the length of the SB and DMV margin; (2) maximal diameter of POC from LAD carina and LCX carina, (3) maximal length of POC from bifurcated carina to the point intersected with the PMV centerline.
3. Area and volume: (1) POC area on 2D images, (2) POC volume on 3D images.

Statistical analysis:

All analyses were performed with statistical software packages (SSPS 20.0, Chicago, IL, USA).

Data were expressed as mean ± SD for continuous or frequency for discrete or categorical variables. To compare differences between groups, student t test was performed for continuous variables, and chi square or Fisher's exact test for the discrete variables. A p value < 0.05 was considered statistically significant.

CTA IMAGING AND ANALYSIS:

Collection of data sets of 100 subjects eligible has been finished (following figure).

Coronary CT angiography (CTA)

- Coronary CT angiography (CTA) is the use of computed tomography (CT)angiography to assess the coronary arteries of the heart

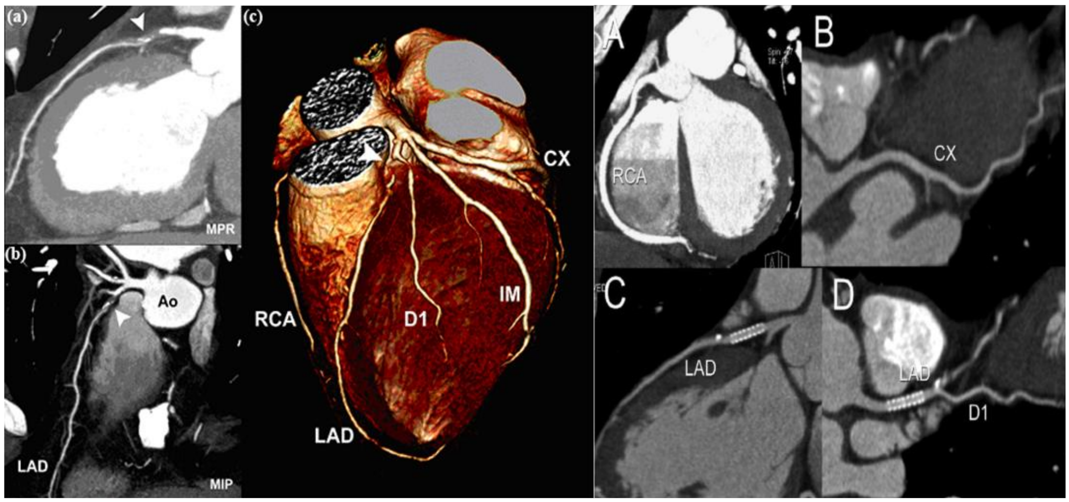

Figure 3: Locations of the bifurcations have been determined

Coronary artery bifurcation

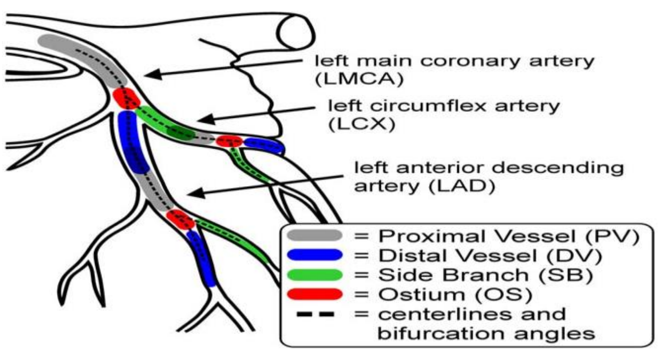

Figure 4: Locations of the bifurcations have been determined

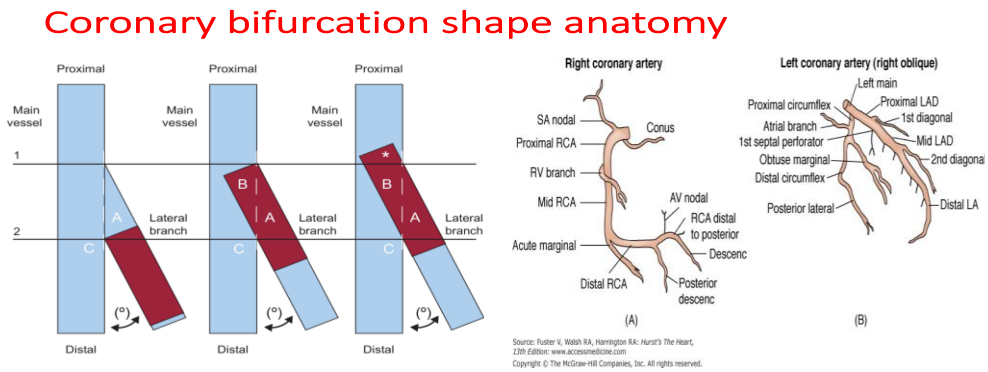

Figure 5: Shapes and types of the bifurcations have been identified

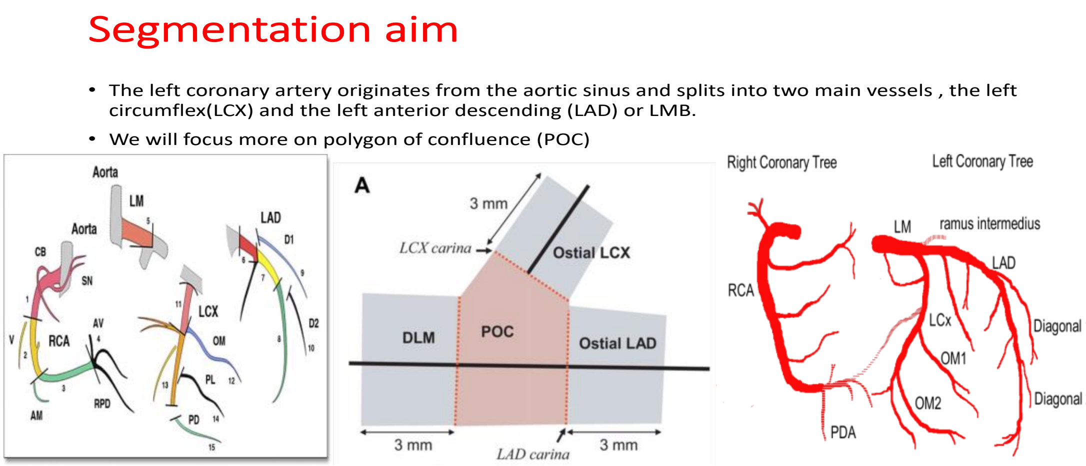

Figure 6: Segmentation of the bifurcations has been set up

Coronary Computed Tomography Angiography (CCTA):

Coronary computed tomography angiography (CCTA) uses an injection of iodine-containing contrast material and CT scanning to examine the arteries that supply blood to the heart and determine whether they have been narrowed. The images generated during a CT scan can be reformatted to create three-dimensional (3D) images that may be viewed on a monitor, printed on film or by a 3D printer, or transferred to electronic media.

Tell your doctor if there's a possibility you are pregnant and discuss any recent illnesses, medical conditions, medications you're taking, and allergies. You will be instructed not to eat or drink anything several hours beforehand and to avoid caffeinated products, Viagra or similar medication. If you have a known allergy to contrast material, your doctor may prescribe medications to reduce the risk of an allergic reaction. These medications must be taken at multiple intervals beginning 13 hours prior to your exam. Leave jewelry at home and wear loose, comfortable clothing. You may be asked to wear a gown. If you are breastfeeding, talk to your doctor about how to proceed.

Coronary computed tomography angiography (CCTA) is a heart imaging test that helps determine if plaque buildup has narrowed the coronary arteries, the blood vessels that supply the heart. Plaque is made of various substances such as fat, cholesterol and calcium that deposit along the inner lining of the arteries. Plaque, which builds up over time, can reduce or in some cases completely block blood flow. Patients undergoing a CCTA scan receive an iodine-containing contrast material as an intravenous (IV) injection to ensure the best possible images of the heart blood vessels.

Computed tomography, more commonly known as a CT or CAT scan, is a diagnostic medical imaging test. Like traditional x-rays, it produces multiple images or pictures of the inside of the body.

The cross-sectional images generated during a CT scan can be reformatted in multiple planes. They can even generate three-dimensional images. These images can be viewed on a computer monitor, printed on film or by a 3D printer, or transferred to a CD or DVD.

CT images of internal organs, bones, soft tissue and blood vessels provide greater detail than traditional x-rays, particularly of soft tissues and blood vessels.

limitations of Coronary CTA:

A person who is very large may not fit into the opening of a conventional CT scanner or may be over the weight limit—usually 450 pounds—for the moving table.

Patients who are extremely overweight or who have abnormal heart rhythms may not be good candidates for this test because image quality may be compromised.

Unlike CCTA, which is only a diagnostic test, invasive coronary angiography can be used for both diagnosis and treatment in a single session. If a narrowing or blockage is found during a CCTA, it cannot be treated at the same time. Patients with a high risk of coronary artery disease and typical symptoms might undergo coronary angiography instead of CCTA because they are more likely to need treatment.

CCTA can be difficult to read if there are many areas of old, calcified (hardened) plaque, which can be the case in older patients.

SEGMENTATION:

The left coronary artery main, also called the left main for short, typically originates at the left aortic sinus of Valsalva and courses in the left anterior direction. After approximately 1 to 2 cm, the left main bifurcates into the left anterior descending artery(LAD) and the circumflex artery (LCX) between the left atrial appendage and the pulmonary trunk.

In our database CTCA LAB, (Fujian. Medical university union hospital), containing over 400 cases, we chose 200 cases of normal study and avoiding third branch trifurcation termed intermediate, arteries with stenosis were excluded from this study.

Typically, the LAD presents one or more child vessels named *diagonals*. Analogously, the LCX gives rise to *obtuse marginals*. We only considered the LAD, LM, POC, first diagonal (D1) and first obtuse marginal (OM1) arteries. A standard operational procedure ensured that the largest branch was labelled as the first obtuse marginal or diagonal. Subsequent branches were identified and labelled but were not included in this bifurcation study. In the right coronary artery, the most important bifurcation from an interventional point of view typically occurs at the *crux* of the heart, splitting into the posterior descending and the postero lateral branches; we refer to this bifurcation as simply the (right-coronary) *crux*.

CTCA scans were semi-automatically segmented as previously described Briefly, a virtual catheter was placed in the left coronary ostium in the CT volumes (Fig. 1). Centerlines were then automatically created and further refined manually. Luminal meshes were generated from these centerlines and the CTCA scans using customized level-set software. All the cases were visually checked for quality and manually labelled. The European Bifurcation Club (EBC) is an academic consortium created in 2004 whose goal has been to assess and recommend the appropriate strategies to manage normal coronary bifurcation in normal population in 2009, the EBC assigned to the angiographic subcommittee the task of developing a consensus regarding the appropriate use of CTCA for the evaluation of bifurcation shape and size in normal population. In Therefore, the aim of this document is to provide an update on the recommendations based on statistical size and shape on normal coronary bifurcation analysis.

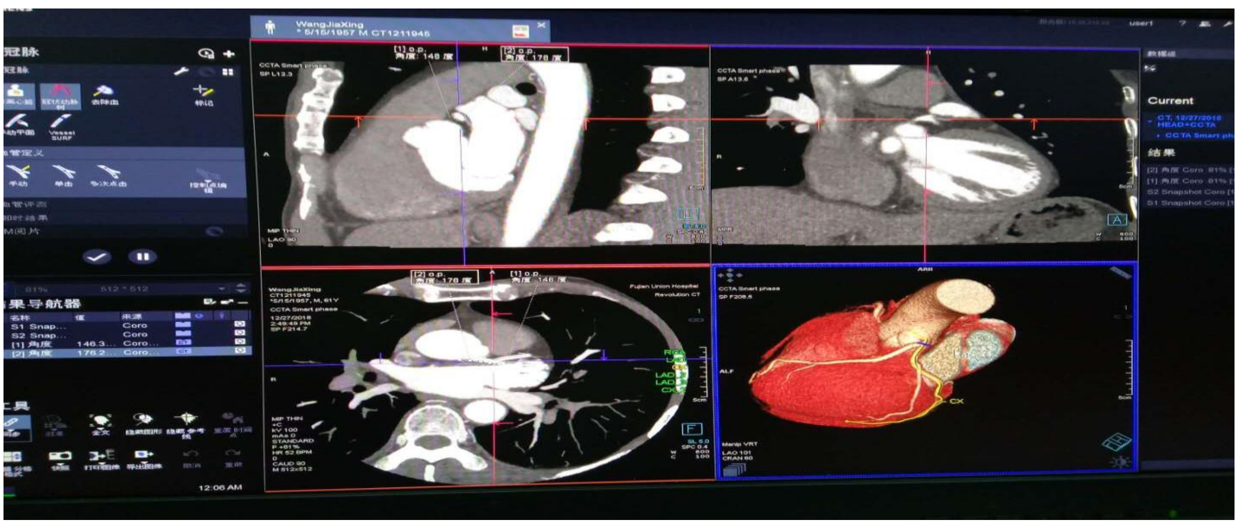

Figure 7: Screen-shot of the segmental tool MIA lite used to extract the luminal mesh from the centerlines and the ct volume, resulting segmentation with the left main bifurcation highlighted in red, units in mm.

3D bifurcation coronary reconstruction from angiographic images Coronary artery disease is the main cause of ischemic heart disease and death in developed countries. Particularly, the treatment of coronary lesions at the bifurcation is a current challenge interventional cardiology. Providing a virtual coronary model and information about stenting implant can represent an important support for the clinical practice, especially for the procedure planning The aim of this study is to implement a method for 3D reconstruction of bifurcation coronary arteries to provide a computer-based tool, having a simple graphical user interface (GUI), devoted to the 3D visualization of the coronary vascular tree and to the calculation of its several geometrical features from two single-plane angiography images [2,3,4]. This elaboration can be further extended for the generation of 3D computational mesh of the vessel wall to be used within structural Finite Element Analysis (FEA). In this study we define a methodological framework, resembling the work- flow depicted in Figure8.

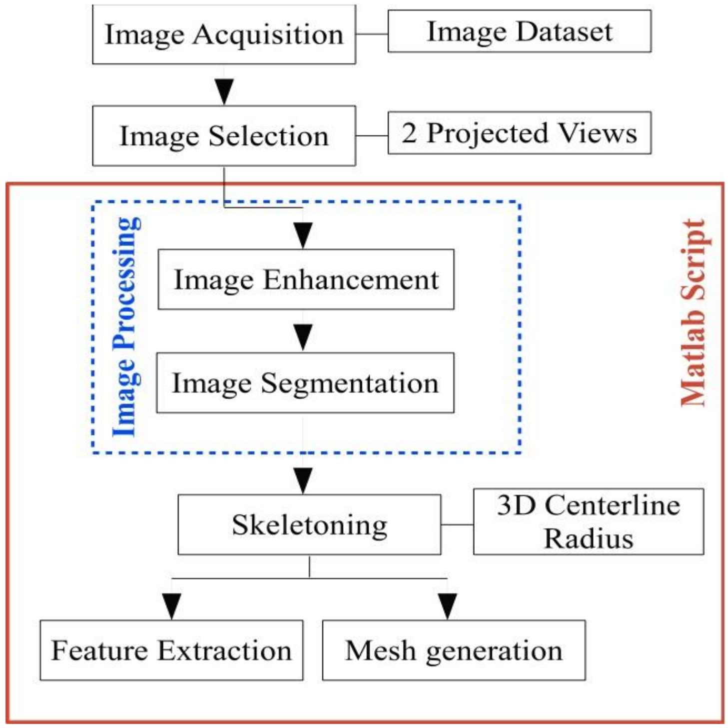

Figure 8: Schematic work-flow of the 3D reconstruction procedure

In the following, we describe briefly each step of the workflow, which is implemented in Matlab (The MathWorks Inc., Natick, MA, USA).

Image enhancement is performed to improve the image quality, removing the noise and enhancing the contrast of the original image.

RESULTS

A total of 200 subjects eligible were included in this study with measurable bifurcations located at the distal LM of 100, LAD-Dx of 150, LCX-OMx of 120, and distal RCA of 120.

1. Parameter measurements

	DBA(°)	Branch diameter (mm)	Marginal length (mm) (mm)	Maximal measurements (mm) (mm) (mm^2)
		PMV DMV SB	DMV-L SB-L	POC-D POC-L POC-A
Distal LM (n=200)	179	4.5±0.8 3.8±1.7 2.8±0.5	3.7±0.9 1.8±0.6	4.1±0.7 4.1±0.7 12.63±0.9

Table 2: Parameters measurements in the distal LM bifurcation

a) Parameter measurements in the different located bifurcations

	DBA(°)	Branch diameter(mm)			Marginal length(mm)		Maximal measurements		
		PMV	DMV	SB	DMV-L	SB-L	POC-D(mm)	POC-L(mm)	POC-A(mm^2)
Distal LM	179°	4.5±0.8	3.8±1.7	2.8±0.5	3.7±0.9	1.8±0.6	4.1±1.2	4.1±0.7	12.63±0.9
LAD-Dx	127°	4.0±0.6	3.3±1.4	2.6±0.7	3.2±0.9	1.6±0.7	3.9±1.0	3.9±0.6	11±0.9
LCX-OMx	170°	3.5±0.5	3.0±2.0	2.4±0.7	2.9±0.9	1.4±0.6	3.2±1.0	3.8±0.7	10.5±0.6
Distal RCA	167°	4.4±2.0	3.2±1.4	2.5±0.7	3.0±0.6	2.5±0.6	4.0±1.0	4.1±0.9	9.5±3.8

Table 3: Parameter measurements in the different located bifurcations

Table 3. Normal coronary bifurcation measurement in the different located bifurcations

Abbreviations: DMV-L = the length of DMV margin of POC; SB-L = the length of SB margin of POC; POC-D = the maximal diameter of POC; POC-L = the maximal length of POC; POC-A = the maximal area of POC (similar in the following table unless otherwise indicated)

2. **Comparison of measurements in the different types of bifurcation**

	DBA(°)	Branch diameter(mm)			Marginal length(mm)		Maximal measurements		
		PMV (LM)	DMV (LM)	SB (LCX)	DMV	SM (LCX)	POC-D (mm)	POC-L (mm)	POC-A (mm^2)
T-type	81°±10	4.3±0.6	3.9±1.7	3.1±0.5	3.8±0.7	1.8±0.6	4.2±0.9	4.1±0.5	13.2±0.9
Y-type	60°±10	4.7±0.5	3.2±1.2	2.6±0.6	1.9±0.5	1.9±0.5	4.3±0.8	4.0±0.5	12.6±0.7

Table 4: Parameter measurements in the different bifurcated types

Table4. Correlation of maximal POC length/diameter to distal bifurcation angle, showed that there was linear relationship between the maximal POC length to distal bifurcation angle (r = x, P<0.001).

From table4 for the Y-type and T-type, the best rule was finet types for both bifurcations whose vessels diameter and bifurcation angels obey finet rule. The mother vessel diameter calculated with the HK rule or Murray is either bigger or smaller than that measured with professional software of CCTA.

The bifurcations from coronary artery were found to obey the finet diameter model and angel rule much more than HK and Murray's model. For distal LM bifurcation the best rule was Finet whose vessels diameters obey Finet rule.

3. **Validation of four rules in different bifurcated types and locations**

	Y bifurcation			T bifurcation		
	HK	FINET	Murray	HK	Finet	Murray
Mother diameter(mm)	3.9	4.0	3.7	4.8	4.7	4.5
Mean diameter of Larger daughter (mm)	3.2	3.2	3.2	3.9	3.9	3.9
Mean diameter of smaller daughter (mm)	2.6	2.6	2.6	3.1	3.1	3.1

Table 5: Parameters for Y and T bifurcated types and locations

Table5. showed that four rules in different bifurcated types and locations.

From table5 we can see for distal LM bifurcation the best rule was Finet whose vessels diameters obey Finet rule. The mother vessel diameter calculated with the HK rule or Murray is either bigger or smaller than that measured with professional software of CCTA. Table5. showed that four rules in different bifurcated types and locations.

For more accurate description of the relationship among three bifurcated segments: for the Y-type and T-type, the best rule was finet types for both bifurcations whose vessels diameter and bifurcation angels obey finet rule

For bifurcations of the distal LM, LAD-Dx, LCX-OMx, and distal RCA, the best rule was finet type whose vessels diameter and bifurcations angel obey finet diameter rule

The bifurcations from coronary artery were found to obey the finet diameter model and angel rule much more than HK and Murray's model.

DISCUSSION

We have presented a coronary bifurcation measurement at different bifurcation locations in normal population based on normal anatomy which is applicable to any collections of shapes and have applied four angel models of coronary diameter bifurcation of 200 patient's models compromising 400 bifurcations in total. Clinical approach to the quantification of vascular bifurcation shape and size focus on diameter and angel with their average diameter measured at different bifurcation location. We did set up a method to detect bifurcation core /polygon of confluence shape and to its dimension in different bifurcation types and locations; we also did validate the four models based on the coronary bifurcation measurement from normal population and we also investigate potential relevance of the BFC/POC morphology in CBLs interventions. As we measure different location of coronary bifurcation, from this study we have stent benefits by forming the size (and future shape) and individual stent selection can be informed. Percutaneous Coronary Intervention is a non-surgical procedure that uses a catheter to place a small structure called a stent to open up blood vessels in the heart that have been narrowed by plaque buildup, a condition known as atherosclerosis. Selection of suitable balloon size for maximal optimization can be ensure by finet diameter rule in comparison to Murray's or HK's rule according to our Finding as you can see in table5 Finet model is more useful than the HK and Murray models for selecting interventional devices and individual stent for PCI. Clinical implication in the different types and locations of bifurcations. There was optimal relationship among the diameters of the three segments of bifurcation, maximal flow through the third segment can be ensure if the normal diameter of first two bifurcations segments are known. Optimal diameter of third segment can be determined to ensure an optimal flow through the bifurcations. It's useful to restore the native bifurcated morphology by current PCI techniques. As for either Y or T type distal left main bifurcation, the Finet diameter model is more suitable than HK's and Murray's model.

CONCLUSION

For more accurate description of the relationship among three bifurcated segments: for the Y-type and T-type, the best rule was finet types for both bifurcations whose vessels diameter and bifurcation angels obey finet rule. The mother vessel diameter calculated with the HK rule or Murray is either bigger or smaller than that measured with professional software of CCTA. For bifurcations of the distal LM, LAD-Dx, LCX-OMx, and distal RCA, the best rule was finet type whose vessels diameter and bifurcations angel obey finet diameter rule The bifurcations from coronary artery were found to obey the finet diameter model and angel rule much more than HK and Murray's model. For distal LM bifurcation the best rule was Finet whose vessels diameters obey Finet rule.

REFERENCES

1. Lassen JF, Holm NR, Banning A, Burzotta F, Lefèvre T, Chieffo A, Hildick-Smith D, Louvard Y, Stankovic G. Percutaneous coronary intervention for coronary bifurcation disease: 11th consensus document from the European Bifurcation Club. EuroInterv. 2016;12(1):38-46.
2. Murray CD. The physiological principle of minimum work. I. The vascular system and the cost of blood volume. Proc Natl Acad Sci.1926;12:207-214
3. Ping Yun Loh J, Anathakrishna R, Kristanto W, et al. Incidence and predictors of target lesion failure in a multi-ethnic Asian population receiving the SYNERGY coronary stent: a prospective all-comers registry. Abstract 1286-179. Presented at: the 66th Annual Scientific Session & Expo of the American College of Cardiology. March 17-19, 2017; Washington, DC
4. Murray CD. The physiological principle of minimum work. II. Oxygen exchange in capillaries. Proc Natl Acad Sci.1926;12:207-214
5. Murray CD. The physiological principle of minimum work applied to the angle of branching of arteries. J Gen Physiol. 1926;9(6):835-41.
6. Zamir M. Distributing and delivering vessels of the human heart. J Gen Physiol. 1988; 91(5):725-35.
7. Zamir M. On Fractal Properties of Arterial Trees. J Theor Biol. 1999;197:517-526
8. Hutchins GM, Miner MM, Boitnott JK. Vessel caliber and branch-angle of human coronary artery branch-points. Circulation Research.1976;38:572-576.
9. Uylings HB. Optimization of diameter and bifurcation angles in lung and vascular tree structures. Bull Math Biol. 1977;39: 509-20.
10. Latib, A, Colombo, A. "Bifurcation disease: what do we know, what should we do?". *JACC Cardiovasc Interv.* vol. 1. 2008. pp. 218-26
11. Gibbons RJ, Abrams J, Chatterjee K, Daley J, Deedwania PC, Douglas JS, Ferguson TB, Fihn SD, Fraker TD, Gardin JM, O'Rourke RA, Pasternak RC, Williams SV, Gibbons RJ, Alpert JS, Antman EM, Hiratzka LF, Fuster V, Faxon DP, Gregoratos G, Jacobs AK, Smith SC; American College of Cardiology, American Heart Association Task Force on Practice Guidelines (Committee on the Management of Patients With Chronic Stable A) . ACC/AHA 2002 guideline update for the management of patients with chronic stable angina—summary article: a report of the American College of Cardiology/American Heart Association Task Force on practice guidelines (Committee on the Management of Patients With Chronic Stable Angina). **Circulation**. 2003; 107:149–158.LinkGoogle Scholar
12. **2**Yasue H, Nakagawa H, Itoh T, Harada E, Mizuno Y. Coronary artery spasm—clinical features, diagnosis, pathogenesis, and treatment. **J Cardiol**. 2008; 51:2–17.CrossrefMedlineGoogle Scholar

13. **3**Nam P, Choi BG, Choi SY, Byun JK, Mashaly A, Park Y, Jang WY, Kim W, Choi JY, Park EJ, Na JO, Choi CU, Lim HE, Kim EJ, Park CG, Seo HS, Oh DJ, Rha SW. The impact of myocardial bridge on coronary artery spasm and long-term clinical outcomes in patients without significant atherosclerotic stenosis. **Atherosclerosis**. 2018; 270:8–12.CrossrefMedlineGoogle Scholar
14. **4**Kim JW, Park CG, Suh SY, Choi CU, Kim EJ, Rha SW, Seo HS, Oh DJ. Comparison of frequency of coronary spasm in Korean patients with versus without myocardial bridging. **Am J Cardiol**. 2007; 100:1083–1086.CrossrefMedlineGoogle Scholar
15. **5**Ong P, Athanasiadis A, Borgulya G, Vokshi I, Bastiaenen R, Kubik S, Hill S, Schaufele T, Mahrholdt H, Kaski JC, Sechtem U. Clinical usefulness, angiographic characteristics, and safety evaluation of intracoronary acetylcholine provocation testing among 921 consecutive white patients with unobstructed coronary arteries. **Circulation**. 2014; 129:1723–1730.LinkGoogle Scholar
16. **6**Choi BG, Park SH, Rha SW, Ahn J, Choi SY, Byun JK, Li H, Mashaly A, Shim MS, Kang JH, Kim W, Choi JY, Park EJ, Lee S, Na JO, Choi CU, Lim HE, Kim EJ, Park CG, Seo HS, Oh DJ. Three-year follow-up of patients with acetylcholine-induced coronary artery spasm combined with insignificant coronary stenosis. **Int J Cardiol**. 2017; 238:66–71.CrossrefMedlineGoogle Scholar
17. Stankovic, G, Darremont, O, Ferenc, M. "Percutaneous coronary intervention for bifurcation lesions: 2008 consensus document from the fourth meeting of the European Bifurcation Club". *EuroIntervention.* vol. 5. 2009. pp. 39-49.
18. Kaimovitz B, Huo Y, Lanir Y, Kassab GS. Diameter asymmetry of porcine coronary vasculature: structural and functional implications. Am J Physiol Heart Circ Physiol. 2008;294:H714-23.
19. Huo Y, Kassab GS. Intraspecific scaling laws of vascular trees. J. R Soc Interface. 2012;9:190-200.
20. Finet G, Gilard M, Perrenot B, et al. Fractal geometry of arterial coronary bifurcations: a quantitative coronary angiography and intravascular ultrasound analysis. EuroInterv. 2008;3:490–498
21. Heart Disease and Stroke Statistics 2017 Update: A Report from the American Heart Association Statistics Committee and Stroke Statistics Subcommittee. *Circulation*. 2017, January 25, http://circ.ahajournals.org/content/early/2017/01/25/CIR.0000000000000485.
22. Finet G, Huo Y, Rioufol G, Ohayon J, Guerin P, Kassab GS. Structure-function relation in the coronary artery tree: from fluid dynamics to arterial bifurcations. EuroInterv. 2010;6 Suppl J:J10-5.
23. Kassab GS, Finet G. Anatomy and function relation in the coronary tree: from bifurcations to myocardial flow and mass. EuroInterv. 2015;11 Suppl V:V13-7.
24. Lassen JF, Burzotta F, Banning AP, Lefèvre T, Darremont O, Hildick-Smith D, Chieffo A, Pan M, Holm NR, Louvard Y, Stankovic G. Percutaneous coronary intervention for the left main stem and other bifurcation lesions: 12th consensus document from the European Bifurcation Club. EuroInterv. 2018 13(13):1540-1553.
25. Burzotta F, Lassen JF, Banning AP, Lefèvre T, Hildick-Smith D, Chieffo A, Darremont O, Pan M, Chatzizisis YS, Albiero R, Louvard Y, Stankovic G. Percutaneous coronary intervention in left main coronary artery

disease: the 13th consensus document from the European Bifurcation Club. EuroInterv . 2018 May 20;14(1):112-120.

26. Gwon HC. Understanding the Coronary Bifurcation Stenting. Korean Circ J. 2018;48 (6):481-491
27. Kang SJ, Ahn JM, Song H, Kim WJ, Lee JY, Park DW, Yun SC, Lee SW, Kim YH, Lee CW, Mintz GS, Park SW, Park SJ. Comprehensive intravascular ultrasound assessment of stent area and its impact on restenosis and adverse cardiac events in 403 patients with unprotected left main disease. Circ Cardiovasc Interv. 2011;4(6):562-9.
28. Beare RJ, Das G, Ren M, Chong W, Sinnott MD, Hilton JE, Srikanth V, Phan TG. Does the principle of minimum work apply at the carotid bifurcation: a retrospective cohort study. BMC Medical Imaging. 2011, 11:17-23.
29. Medrano-Gracia P, Ormiston J, Webster M, Beier S, Young A, Ellis C, Wang C, Smedby Ö, Cowan B. A computational atlas of normal coronary artery anatomy. EuroInterv. 2016;12 (7):845-54.
30. Medrano-Gracia P, Ormiston J, Webster M, Beier S, Ellis C, Wang C, Smedby Ö, Young A, Cowan B. A Study of Coronary Bifurcation Shape in a Normal Population. J Cardiovasc Transl Res. 2017;10(1):82-90.
31. Sakellarios A, Bourantas CV, Papadopoulou SL, Kitslaar PH, Girasis C, Stone GW, Reiber JHC, Michalis LK, Serruys PW, de Feyter PJ, Garcia-Garcia HM, Fotiadis DI. The effect of coronary bifurcation and haemodynamics in prediction of atherosclerotic plaque development: a serial computed tomographic coronary angiographic study. EuroInterv. 2017 Oct 13;13(9):e1084-e1091.
32. Antoniadis AP, Giannopoulos AA, Wentzel JJ, Joner M, Giannoglou GD, Virmani R, Chatzizisis YS. Impact of local flow haemodynamics on atherosclerosis in coronary artery bifurcations. EuroInterv. 2015;11 Suppl V:V18-22.
33. Doutel E, Pinto SI, Campos JB, Miranda JM. Link between deviations from Murray's Law and occurrence of low wall shear stress regions in the left coronary artery. J Theor Biol. 2016;402:89-99.
34. Chen HY, Moussa ID, Davidson C, Kassab GS. Impact of main branch stenting on endothelial shear stress: role of side branch diameter, angle and lesion. J R Soc Interface. 2012;9(71):1187-93.
35. Gonzalo N, Garcia-Garcia HM, Regar E, Barlis P, Wentzel J, Onuma Y, Ligthart J, Serruys PW. In vivo assessment of high-risk coronary plaques at bifurcations with combined intravascular ultrasound and optical coherence tomography. JACC Cardiovasc Imaging. 2009;2(4):473-82.
36. Oviedo C, Maehara A, Mintz GS, Araki H, Choi SY, Tsujita K, Kubo T, Doi H, Templin B, Lansky AJ, Dangas G, Leon MB, Mehran R, Tahk SJ, Stone GW, Ochiai M, Moses JW. Intravascular ultrasound classification of plaque distribution in left main coronary artery bifurcations: where is the plaque really located? Circ Cardiovasc Interv. 2010;3(2):105-12.
37. Li QH, Zhang Q, Li XL, Yin JF, Ji HG. A volumetric intracoronary ultrasonographic study of coronary bifurcation lesions. Eur Rev Med Pharmacol Sci. 2018;22(4):1094-1101.
38. Ellwein L, Marks DS, Migrino RQ, Foley WD, Sherman S, LaDisa JF Jr. Image-based quantification of 3D morphology for bifurcations in the left coronary artery: Application to stent design. Catheter Cardiovasc Interv. 2016;87(7):1244-55.

39. Antoniadis AP, Mortier P, Kassab G, Dubini G, Foin N, Murasato Y, Giannopoulos AA, Tu S, Iwasaki K, Hikichi Y, Migliavacca F, Chiastra C, Wentzel JJ, Gijsen F, Reiber JH, Barlis P, Serruys PW, Bhatt DL, Stankovic G, Edelman ER, Giannoglou GD, Louvard Y, Chatzizisis YS. Biomechanical Modeling to Improve Coronary Artery Bifurcation Stenting: Expert Review Document on Techniques and Clinical Implementation. JACC Cardiovasc Interv. 2015;8(10):1281-96.
40. Hu F, Tu S, Cai W, Jiang Z, Zheng H, Xiao L, Qiu C, Xiong C, Yao Y, Chen L. Double kissing mini-culotte versus mini-culotte stenting: insights from micro-computed tomographic imaging of bench testing. EuroIntervention. 2018 Dec 11. [Epub ahead of print]
41. Derimay F, Souteyrand G, Motreff P, Guerin P, Pilet P, Ohayon J, Darremont O, Rioufol G, Finet G. Sequential Proximal Optimizing Technique in Provisional Bifurcation Stenting With Everolimus-Eluting Bioresorbable Vascular Scaffold: Fractal Coronary Bifurcation Bench for Comparative Test Between Absorb and XIENCE Xpedition. JACC Cardiovasc Interv. 2016;9(13):1397-406.
42. Finet G, Derimay F, Motreff P, Guerin P, Pilet P, Ohayon J, Darremont O, Rioufol G. Comparative Analysis of Sequential Proximal Optimizing Technique Versus Kissing Balloon Inflation Technique in Provisional Bifurcation Stenting: Fractal Coronary Bifurcation Bench Test. JACC Cardiovasc Interv. 2015;8(10):1308-17.
43. Rahman S, Leesar T, Cilingiroglu M, Effat M, Arif I, Helmy T, Leesar MA. Impact of kissing balloon inflation on the main vessel stent volume, area, and symmetry after side-branch dilation in patients with coronary bifurcation lesions: a serial volumetric intravascular ultrasound study. JACC Cardiovasc Interv. 2013 Sep;6(9):923-31.
44. Collet C, Onuma Y, Cavalcante R, Grundeken M, Généreux P, Popma J, Costa R, Stankovic G, Tu S, Reiber JHC, Aben JP, Lassen JF, Louvard Y, Lansky A, Serruys PW. Quantitative angiography methods for bifurcation lesions: a consensus statement update from the European Bifurcation Club. EuroInterv. 2017;13(1):115-123.
45. Girasis C, Schuurbiers JC, Muramatsu T, Aben JP, Onuma Y, Soekhradj S, Morel MA, van Geuns RJ, Wentzel JJ, Serruys PW. Advanced three-dimensional quantitative coronary angiographic assessment of bifurcation lesions: methodology and phantom validation. EuroInterv. 2013;8(12):1451-60.
46. Grundeken MJ, Ishibashi Y, Ramcharitar S, Tuinenburg JC, Reiber JH, Tu S, Aben JP, Girasis C, Wykrzykowska JJ, Onuma Y, Serruys PW. The need for dedicated bifurcation quantitative coronary angiography (QCA) software algorithms to evaluate bifurcation lesions. EuroInterv. 2015;11 Suppl V:V44-9.
47. Kern MJ, Seto AH. Bifurcation lesion assessment with advanced quantitative coronary angiography: A method still wanting. Catheter Cardiovasc Interv. 2018;91(7):1271-1272